Biomedical Signal Processing and Control 82 (2023) 104560

Contents lists available at ScienceDirect

Biomedical Signal Processing and Control

journal homepage: www.elsevier.com/locate/bspc

Variational mode decomposition for surface and intramuscular EMG signal denoising

H. Ashraf [a], U. Shafiq [b], Q. Sajjad [b], A. Waris [b,*], O. Gilani [b], M. Boutaayamou [a], O. Brüls [a]

[a] Laboratory of Human Motion Analysis, University of Liège (ULiège), Liège, Belgium
[b] Department of Biomedical Engineering and Sciences, School of Mechanical and Manufacturing Engineering (SMME), National University of Science and Technology (NUST), 44000 Islamabad, Pakistan

ARTICLE INFO

Keywords:
EMG signal denoising
Intramuscular EMG
Variational mode decomposition

ABSTRACT

Electromyographic signals contaminated with noise during the acquisition process affect the results of follow-up applications such as disease diagnosis, motion recognition, gesture recognition, and human–computer interaction. This paper proposes a denoising technique based on the variational mode decomposition (VMD) for both surface electromyography signals (sEMG) and intramuscular electromyography signals (iEMG). sEMG and iEMG obtained from 5 healthy subjects were first decomposed using VMD into respective variational mode functions (VMFs), then thresholds were set to remove the noise, and finally, the denoised signal was reconstructed. The denoising efficacy of interval thresholding (IT) and iterative interval thresholding (IIT) techniques in combination with SOFT, HARD, and smoothly clipped absolute deviation (SCAD) thresholding operators was quantitatively evaluated by using Signal to Noise Ratio (SNR) and further statistically validated by Friedman test. The results demonstrated that IIT provides better SNR values than IT at all noise levels (P-value < 0.05) for sEMG signals. For iEMG, IIT outperformed IT at 0db and 5db noise levels, but at a noise level of 10db and 15db, IT outperformed IIT. However, the results for the 10db noise level were statistically insignificant. The SOFT thresholding operator outperforms HARD and SCAD at all noise levels for sEMG, as well as iEMG (P-value $<$ 0.05). The study demonstrates that the combination of the IIT thresholding technique with the VMD-based SOFT thresholding operator yields the best denoising results while retaining the original signal characteristics. The proposed method can be used in the fields of disease diagnosis, pattern recognition, and movement classification.

1. Introduction

The Electromyographic (EMG) signal is the electrical realization of a contracting muscle coupled with neuromuscular stimulation. The signal reflects the current produced by ionic movement through the membrane of the muscle tissue that perpetuates reaching the sensing area of a recording electrode located in the environment through the intervening tissues [1]. EMG signals recorded noninvasively from the skin surface are referred to as surface EMG (sEMG) signals, whereas the signals recorded invasively directly from the muscles are referred to as intramuscular EMG (iEMG) signals. Both sEMG and iEMG signals are widely used in a range of clinical, diagnostic, and rehabilitative applications [2].

Due to differences in recording techniques for sEMG and iEMG signals, their inherent characteristics differ. Based on these characteristic differences, their associated application area also differs [3]. The applications of iEMG signals remained obscured by the convenient use of sEMG signals. However, with technological advancements and the development of implantable electrode arrays, the use of iEMG signals is now being considered in a much greater way. Due to their noninvasive recordings, sEMG signals are widely used in rehabilitation engineering to design and control rehabilitative and assistive devices [4] as well as in applications such as gesture recognition [5]. iEMG signals are mostly used for detection and disease diagnosis in clinical applications [6]. The accuracy and performance of any EMG-based application are compromised and affected by the presence of unwanted noise. Various types of noise adversely affect the quality of the signal, making it difficult to use EMG signals for any application. Therefore, minimizing unwanted noise from EMG signals is a serious issue to be considered. Conventional filters are widely used to minimize the effect of unwanted noise embedded in the original signal such as low pass, high pass, adaptive, Wiener and Kalman filters, etc. [7]. Although traditional filters remove a significant

* Corresponding author.
E-mail address: asim.waris@smme.nust.edu.pk (A. Waris).

https://doi.org/10.1016/j.bspc.2022.104560
Received 3 August 2022; Received in revised form 16 December 2022; Accepted 26 December 2022
Available online 4 January 2023

portion of noise from the signal but do not preserve the original characteristics of the signal since the frequencies in-common with the noise are also removed.

To address the issue of preservation of the original characteristics of the EMG signal, wavelet denoising methods based on the wavelet transform of the signal were introduced [8,9]. In the case of iEMG signals, the wavelet transforms along with ICA decomposition have been utilized for denoising [10]. Advanced denoising technique such as Multiscale principal component analysis that also operates based on wavelet transform has also been used for denoising of iEMG signals [11]. The performance of the wavelet transform is much better compared to that of conventional filtering techniques. However, the selection of a predefined mother wavelet function greatly influences the results [9]. Huang et al. (1994) proposed a data-focused and entirely adaptive signal decomposition method, 'empirical mode decomposition (EMD)' [12]. The advantage of EMD is that it does not make any assumptions about the data and the signal remains in the time domain throughout the decomposition method [13]. Whereas in wavelet-based denoising techniques, the signal is converted to frequency domain for the analysis of the signal, and most of these techniques assume that the data are stationary. EMG signals are stochastic and non-stationary in nature. EMD-based signal denoising techniques have been proposed to denoise the input signal. EMD decomposes the input signal into its Intrinsic Mode Functions (IMF), by recursively detecting local extrema values which are then used, using interpolation, to find upper and lower envelopes in the signal [14]. It isolates the high-frequency components or oscillations by averaging envelopes as the low-pass centerline. The only drawback of EMD-based denoising techniques is the mode mixing of IMFs and the dependence of decomposition on different techniques of interpolation and extrema finding [13]. Due to these limitations, the EMD has a high sensitivity to sampling and noise. To address the issue of mode mixing, various versions of EMD have been proposed, such as ensemble empirical mode decomposition (EEMD) [15], complete ensemble empirical mode decomposition (CEEMD) [16], and complete ensemble empirical mode decomposition with additive noise (CEEMDAN). However, these decomposition methods do not completely solve the mode-mixing problem and are computationally expensive [15,16].

Dragomiretskiy et al. (2014) introduced the variational mode decomposition (VMD) by generalizing the Wiener filter into various adaptive bands [17]. VMD is a fully adaptive intrinsic signal decomposition method whose minimization governs the decomposition of a given signal into its variational mode functions (VMF). Each obtained VMF is smooth after demodulation and has its unique central frequency. To avoid mode mixing in VMD, the components of each VMF are obtained concerning the frequency domain of the signal. VMD-based denoising has been successfully applied for seismic time–frequency analysis, for the detection of gearbox fault diagnosis [18], wind speed forecasting [19], bearing fault diagnosis [20], denoising of biomedical images [21], ECG and EMG signal denoising [22,23]. Xiao et al. (2019) proposed a new SOFT iterative thresholding-based VMD (SIT-VMD) to denoise sEMG signals in comparison with wavelet and EMD-based denoising methods [23]. Ma et al. (2020) utilized VMD with a wavelet sub-band thresholding technique to effectively denoise the sEMG signals [24]. The authors first introduced the artificial white gaussian noise (WGN) into experimentally recorded EMG signal, and then by using a wavelet-based SOFT thresholding operator the denoising of the signals was performed using VMD. The authors reported that the VMD-based denoising technique outperforms wavelet, EMD, and EEMD-based denoising methods to denoise sEMG signals. Research by Xiao et al. (2019) and Ma et al. (2020) shows that VMD has great potential to denoise EMG signals. However, both studies were conducted on sEMG signals and the potential of both EMD and VMD-based denoising methods for iEMG signals is yet to be explored.

Power line interference (PLI), white gaussian noise (WGN), and baseline wandering (BW) are the most common types of noise that contaminate the EMG signals [25–27]. Most of the current time–frequency domain literature regarding the denoising of EMG signals focuses only on sEMG signals and the removal of WGN [23]. In this study, for the first time, the potential of time–frequency domain decomposition-based denoising techniques has been explored for both iEMG and sEMG signals. Furthermore, a novel VMD-based signal denoising framework that is equally effective for sEMG and iEMG signals to eliminate PLI, WGN, and BW has been proposed. The proposed method utilized VMD to decompose the input signal into its subsequent VMF, and then iterative interval thresholding is applied to each VMF. The proposed method is termed iterative interval variational mode decomposition (IIT-VMD). To demonstrate the capabilities of the proposed method, 15 sEMG and 15 iEMG recordings were used. The dataset is made up of both sEMG and iEMG signals recorded from 5 healthy subjects in which the data for each subject were recorded in three sessions, making the total number of recordings 30.

The rest of the paper is structured as follows: Section II outlines the origins of the dataset, the suggested denoising process, the measurement criteria, and the parameter selection. The findings of both sEMG and iEMG cases are explained in Section 3. The output of four denoising methods is evaluated in Section 4, and the conclusions are given in Section 5.

2. Methodology

A. Dataset

Data from 5 healthy male participants with no injury or disability were collected. All subjects were between the age of 20 and 56 years (mean $\pm$ std $=$ 31 $\pm$ 4 years). The data comprise both sEMG and iEMG signals. Before carrying out the experimental procedure, written consent was obtained from the subjects. Approval no.: ref#NUST/SMME-BME/REC/000129/20012019 was granted by the local ethical committee of the National University of Science and Technology, Islamabad, Pakistan for data recording.

B. Experimental setup

Six bipolar Ag/AgCl electrodes (Ambu WhiteSensor 0415M) were used for the recording of sEMG data concurrently with six Teflon-coated stainless steel electrodes (A-M Systems, Carlsborg WA diameter 50 μm) for iEMG data as shown in Fig. 1. The data were collected from the dominant upper limb of the subjects. The forearm muscles used are the following: Extensor Carpi Radialis, Extensor Digitorum Muscle, Extensor Carpi Ulnaris, Flexor Carpi Radialis, Palmaris Longus, and Flexor Digitorum Superficialis.

The area of interest was prepared by cleaning with an alcohol swab and shaving off the excessive hair. sEMG electrodes were placed on the skin surface above the belly of the muscle, perpendicular to the muscle fiber. Just underneath the sEMG electrode pairs, sterile intramuscular wire electrodes, with an exposed tip up to 3 mm [28], were inserted into the muscle using a hypodermic needle by penetrating the skin up to 10–15 mm. The needle was then removed, with the wire electrodes left in the muscle. Precautionary measures were taken to prevent electrode contamination. The insertion sites were covered with bandages to restrict unnecessary movement, leaving the tips of the electrodes outside for communication between the electrodes and the amplifiers. EMG signals were amplified (AnEMG12, OT Bioelectronica, Torino, Italy), filtered analog bandpass (10–500 Hz for sEMG and 100–1900 Hz for iEMG), and sampled at 8 kHz (16-bit NI-DAQ PCI-6221).

C. Preprocessing

Six EMG signals were recorded from each subject. Five-second contractions were repeated four times in each session. The subject went from rest to a medium-level contraction, holding it for a period of three seconds. An open-source software i.e. BioPatRec (Oritz-Catalan, 2014), prompted the subject for each motion by displaying a selection of images. Each contraction was followed by a rest period at the same time to avoid muscle fatigue. The recorded data were first passed through a third-order Butterworth bandpass filter. The bandpass filter for the sEMG signal had a lower and upper cutoff frequency of 4 Hz and 500 Hz.

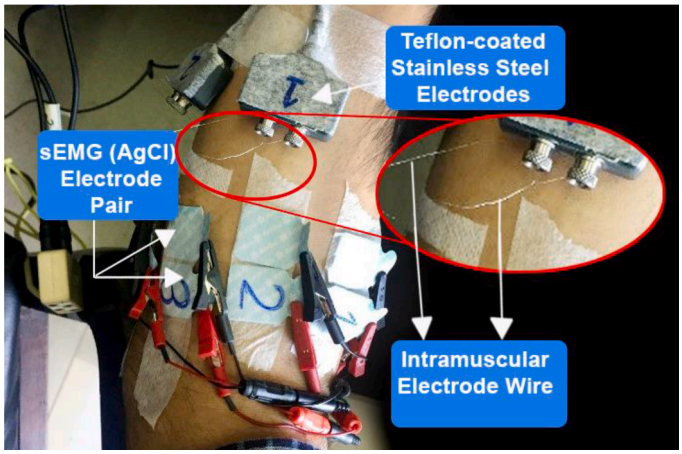

Fig. 1. An illustration of the experimental setup.

The bandpass filter implemented on iEMG had a lower cut-off frequency of 10 Hz and a higher cut-off frequency of 1500 Hz. To reduce the power-line interference, the filtered sEMG and iEMG signals were passed through a notch filter at 60 Hz. The magnitude response of the notch filter is shown in Fig. 2.

Fig. 3 depicts examples of original sEMG and iEMG signals along with their respective frequency spectrums. After removing the power-line interference the signals are introduced to artificial white Gaussian noise as governed by (1)

$$f = \bar{f} + \sigma \bullet n(t) \tag{1}$$

where $\bar{f}$ is the original signal and f is the resultant noisy signal due to the addition of noise σ(t).

The overall methodology is shown in Fig. 4.

D. Variational Mode Decomposition.

The VMD method can separate harmonic signals of close frequency range without any effect from the sampling frequency, thus avoiding mode mixing. VMD is a generalized form of the wiener filter into multiple adaptive bands [14]. The estimated model and the corresponding center frequency are updated consistently, making the model estimation variational. After each estimation, the model is translated into the time domain by the use of the inverse Fourier transform.

VMD decomposes the original signal into a discrete number of sub-signals called VMFs given by:

$$f = \sum_{k=1}^{M} \mu^k \tag{2}$$

where μ^k is the sub-signal of the original signal f, M is the number of modes and μ^k(t) is defined as:

$$\mu^k(t) = a^k(t) \bullet cos\left(\varphi^k(t)\right) \tag{3}$$

where $a^k(t)$ represents the envelope of the signals,and $\varphi^k(t)$ is the phase

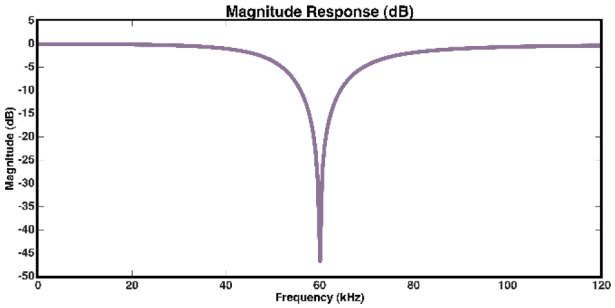

Fig. 2. Magnitude response of the notch filter (cut-off frequency: 60 Hz).

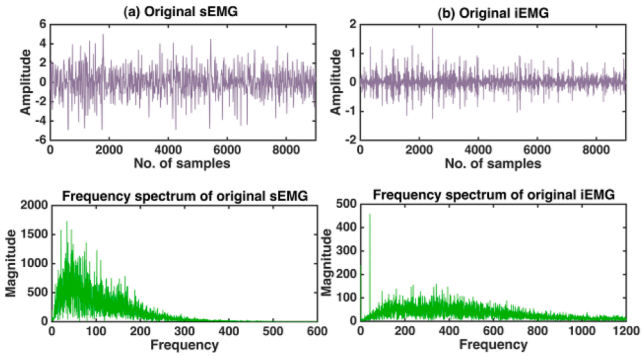

Fig. 3. (a) Original sEMG signal with its frequency spectrum, and (b) Original iEMG signal with its frequency spectrum.

of the signal. In addition to the noise, (2) becomes:

$$f = \bar{f} + \Delta = \sum_{k=1}^{M} \mu^k + r^n \tag{4}$$

here μ^k, r^n, $\bar{f}$, and Δ represent sub-signals obtained from f, the remainder term, the original signal, and the added noise respectively. According to Equation (4), the summation of VMFs will result in the input signal. A central frequency ω_k with limited bandwidth is associated with each VMF. It can be determined by decomposition and using (4). To determine the bandwidth, an analytic signal representation is computed that exhibits a unilateral frequency. Then the resultant unilateral spectrum is shifted via harmonic mixing with complex frequency exponential. Finally, the squared norm of the gradient of the resulting signal is acquired.

Considering these steps, the associated optimization problem becomes:

$$min_{\{u_k\},\{w_k\}} \left| \left\{ \sum_k \left\| \partial_t \left[\left(\delta(t) + \frac{j}{\pi t} \right) * u_k(t) \right] e^{-jw_k t} \right\|_2^2 \right\} \right.$$

$$s.t. \sum_k u_k = f \tag{5}$$

The operator is L^2 is the squared norm of the expression and the expression $\left(\delta(t) + \frac{j}{\pi t}\right) * u_k(t)$ is the Hilbert transform of $u_k(t)$, transforming $u_k(t)$ into the analytic signal. This is done to achieve a one-sided frequency spectrum with only positive frequencies.

The use of a quadratic penalty factor and the exponential Lagrangian multiplier changes the constraint variation problem to a non-constraint variation problem given by (6).

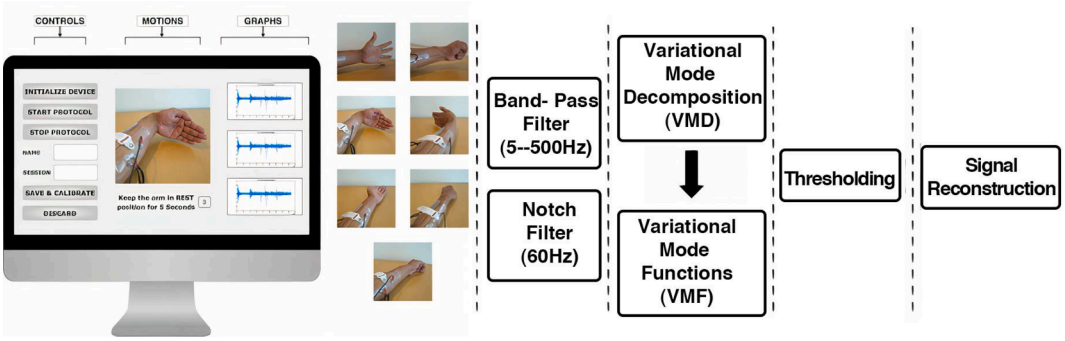

Fig. 4. Block diagram for the proposed method for signal denoising.

$$L(\{u_k\},\{w_k\},\lambda) = \alpha\sum_k \left\| \partial_t \left[\left(\delta(t) + \frac{i}{\pi t}\right) * u_k(t) \right] e^{ijw_k t} \right\|_2^2 + \|f(t) - \sum_k u_k(r)\|_2^2 + \left\langle \lambda(t), f(t) - \sum_k u_k \right\rangle \quad (6)$$

Here α is the regularization term. The quadratic penalty factor guarantees the accuracy of the reconstructed signal. The Lagrangian multiplier keeps the constraint condition strict. The complete optimization problem is solved using the alternate direction method of multipliers (ADMM) in which the problem is solved as a sequence of iterative sub-optimization problems as expressed in (7). The purpose of these sub-problems is to minimize the cost function iteratively for the parameter of interest [29,30].

$$u_k^{n+1} = \arg min_{u_k \in X} \left\{ \alpha \| \partial_t \left[\left(\delta(t) + \frac{j}{\pi t}\right) * u_k t \right] e^{ijw_k t} \|_2^2 + \|f(t) - \sum_i u_i(t) + \frac{\lambda(t)}{2}\|_2^2 \right\} \quad (7)$$

This is solved by using the Parseval/Plancherel Fourier Isometry method that transforms (7) from the time domain to the frequency domain:

$$\hat{u}_k^{n+1}(w) = \frac{f(w) - \sum_{i\neq k} \hat{u}_i(w) + \frac{\hat{\lambda}(w)}{2}}{1 + 2\alpha(w - w_k)^2} \quad (8)$$

$$w_k^{n+1} = \frac{\int_0^\infty w|\hat{u}_k(w)|^2 dw}{\int_0^\infty |\hat{u}_k(w)|^2 dw} \quad (9)$$

$$\hat{\lambda}^{n+1}(w) \leftarrow \hat{\lambda}^n(w) + \tau\left(\hat{f}(w) - \sum \hat{u}_k^{n+1}(w)\right) \quad (10)$$

Here τ represents noise tolerance.

A criterion needs to be established to stop the iterations. Iterations stop if (11) is satisfied for a given discrimination accuracy. As a result, we can acquire K narrow-band VMF components. The distinctive VMD procedure is highlighted in Fig. 5.

$$\frac{\sum_k \left\| \hat{u}_k^{n+1} - \hat{u}_k^n \right\|_2^2}{\|\hat{u}_k^n\|_2^2} < \varepsilon \quad (11)$$

After the signal decomposition, several corresponding VMFs are used to reconstruct the required signal. To select these VMFs, the Hilbert transformation can be used to calculate the frequency of each VMF based on the center frequency and the limited bandwidth frequency as given in (12). The required VMFs for the reconstruction of each signal are then selected based on the frequencies.

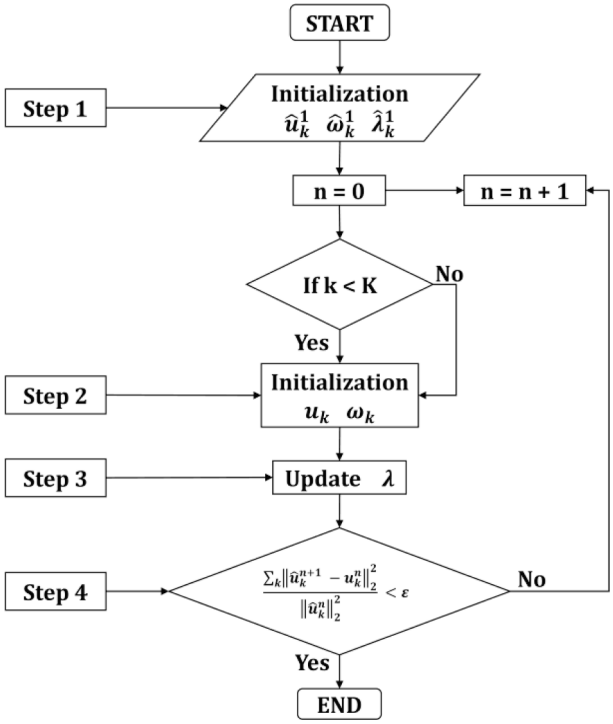

Fig. 5. Flowchart for Variational Mode Decomposition Algorithm.

$$H(f,t) = Re\sum_{i=1}^{n} a_i(t) e^{j2\pi \int u_i t)dt} \quad (12)$$

E. Thresholding Techniques and Operators.

Time-frequency denoising techniques are inspired by wavelet domain denoising techniques. Due to the resemblance of the decomposed VMFs with Amplitude-Modulated or Frequency-Modulated signals, the mean of each VMF is zero. Thus, direct application of wavelet-like thresholding, SOFT or HARD will give inaccurate results. The denoising of each VMF is carried out by a combination of wavelet domain thresholding operators HARD, SOFT, and smoothly clipped absolute deviation (SCAD) along with different thresholding techniques.

HARD thresholding sets the coefficients with values lower than a predefined threshold (T) to zero. In HARD thresholding, the coefficients above T remain unchanged. The reconstructed signal after HARD thresholding exhibits discontinuities [27]. To overcome this disadvantage, SOFT thresholding is used. SOFT thresholding uses the absolute values of the coefficients. Coefficients with absolute values lower than T are set to zero. The remaining non-zero values are shifted towards zero by an amount T, thus, introducing a bias in the reconstructed signal. To avoid unnecessary bias, the SCAD penalty sets the smaller coefficients to

zero, shrinks a few coefficients towards zero, and keeps the larger coefficients as they are. Mathematically SOFT, HARD and SCAD can be represented as (13), (14), and (15) respectively.

$$f(u_k) = \begin{cases} sgn(u_k)(|u_k| - T), |u_k| \rangle T \\ 0, |u_k| \le T \end{cases} \tag{13}$$

$$f(u_k) = \begin{cases} u_k, |u_k| \rangle T \\ 0, |u_k| \le T \end{cases} \tag{14}$$

$$f(u_k) = \begin{cases} sgn(y)\max(0, |u_k| - T), |u_k| \le 2T \\ \dfrac{(z-1)u_k - zT(sgn(u_k))}{z-2}, 2T < |u_k| \le zT \\ u_k, |u_k| > zT \end{cases} \tag{15}$$

where u_k is the obtained VMF from the VMD process explained in the previous section. The value of z is recommended to be 3.7 according to the Bayesian argument [31].

The value of T is kept more than the maximum noise level present in the noisy signal [32,33]. The value of T is selected by:

$$T = \sigma\sqrt{2\log_e N} \tag{16}$$

where N gives the corresponding signal length and σ represents the level of noise. σ can be calculated by (17).

$$\sigma_i = \frac{median(|u_i(t)|)}{0.6745} \tag{17}$$

Interval thresholding (IT) is applied on an interval of zero crossings between u_k and u_{k+1}, in combination with HARD, SOFT, and SCAD operator can be mathematically represented as (18), (19) and (20) respectively.

$$\widetilde{p}_j^i = \begin{cases} p_j^{(i)}, \left|q_j^{(i)}\right| \rangle T_i \\ 0, \left|q_j^{(i)}\right| \rangle T_i \end{cases} \tag{18}$$

$$\widetilde{p}_j^i = \begin{cases} p_j^{(i)} \dfrac{\left|q_j^{(i)}\right| - T_i}{|q_j^{(i)}|}, \left|q_j^{(i)}\right| > T_i \\ 0, \left|q_j^{(i)}\right| \le T_i \end{cases} \tag{19}$$

$$\widetilde{p}_j^i = \begin{cases} p_j^{(i)} \dfrac{\max\left(0, \left|q_j^{(i)}\right| - T_i\right)}{|q_j^{(i)}|}, \left|q_j^{(i)}\right| > T_i \\ p_j^{(i)} \dfrac{(z-1)\left(0, \left|q_j^{(i)}\right| - zT_i\right)}{|q_j^{(i)}|}, 2T_i < \left|q_j^{(i)}\right| \le zT_i \\ 1, \left|q_j^{(i)}\right| \rangle zT_i \end{cases} \tag{20}$$

Here $j = 1, 2 \ldots Nz_i$, where *Nzi* is the *Nth* zero crossing in ith IMF. $p_j^{(i)}$, $p_j{}^i$ and $q_j^{(i)}$ represent noisy signal, thresholded values and maximum values of noisy signal respectively, between instants u_j *(i)* to u_{j+1}*(i)* of the i^{th} IMF.

The drawback of IT is its sensitivity to noise, which can be overcome by using IIT. IIT achieves several approximations of the denoised signal iteratively using IT and averages them, resulting in higher noise tolerance [31]. These versions are produced by the decomposition of various noisy versions of the input VMF. The coefficients of the first VMF are randomly shuffled in the next approximation of the noisy signal. The unchanged decomposed VMFs and shuffled VMFs are added together to get a new approximation of the signal. This method is carried out iteratively to get the required number of approximations. Each approximation is denoised using IT. The denoised versions are averaged to get the final denoised signal with higher noise tolerance.

F. Performance Evaluation.

The selected evaluation metrics for the evaluation of the performance of the implemented method were the signal-to-noise ratio (SNR) and the root mean squared error (RMSE) which are widely used to evaluate the performance of the signal filtering techniques. To make a fair comparison, the SNR value and RMSE value were calculated for the original signal and the noisy signal after the introduction of artificial noise. SNR and RMSE values were calculated using (21) and (22) respectively.

$$SNR = 10 \bullet \log_{10}\left(\frac{\sum\left(f(t)^2\right)}{\sum\left(\left(\bar{f}(t) - f(t)\right)^2\right)}\right) \tag{21}$$

$$RMSE = \sqrt{\frac{1}{L}\sum\left(f(t) - \bar{f}(t)\right)^2} \tag{22}$$

where $f(t)$ is the original signal and $\bar{f}(t)$ is the denoised signal. The results obtained were validated by comparing mean ranks between all the groups collectively and between the related groups for multiple comparisons using Friedman's nonparametric test.

3. Results

EMG data from 5 participants are used to test the efficacy of the denoising performance. After the decomposition of EMG signal thresholding techniques, IT, IIT, and three thresholding operators SOFT, HARD, and SCAD are applied for denoising. EMG signals are non-stationary and stochastic in nature, thus the noise was introduced at various noise levels of 0db, 5db, 10db, and 15db as shown in Fig. 6.

G. VMD Denoising

VMD is used to divide the signal into subsequent VMFs. Fig. 7 shows an example of sEMG and iEMG signal decomposed into their corresponding VMFs represented by VMF_1-VMF_n where n is the total number of VMFs. Each VMF contains a range of frequencies present in the original signal. Fig. 8 shows the corresponding frequency spectrum of the VMFs with a center frequency and a narrow frequency band for each VMF. As evident from Fig. 8, VMF_1 contains the highest frequency range thus comprising the highest amount of noise. The lower frequencies can be observed in the higher VMFs depicting a lower amount of noise.

It can be seen from Fig. 8 that frequency bands are converging as the order of VMFs increases. The narrower frequency band of the VMFs is beneficial in the subsequent signal-filtering process. These decomposed models can be used to reconstruct the original signal.

H. Comparison of VMD Denoising Performance.

A lot of denoising methods have been proposed by different researchers based on EMD and VMD for sEMG signals but no literature has been found for denoising iEMG signals using those methods. Before VMD, EMD with IT and SOFT thresholding operators had been proposed as the optimal method to eliminate various types of noise for sEMG

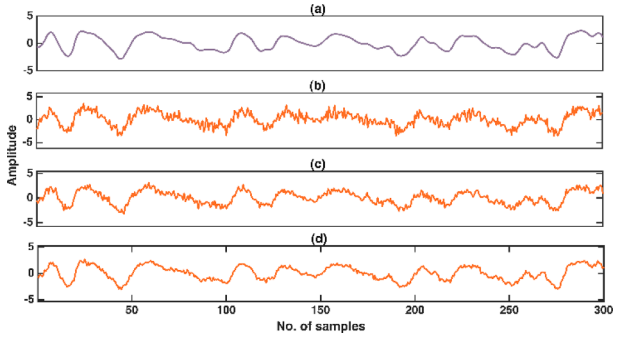

Fig. 6. (a) Original EMG signal, (b) signal with 5 dB noise, (c) Signal with 10 dB noise, (d) Signal with 15 dB noise.

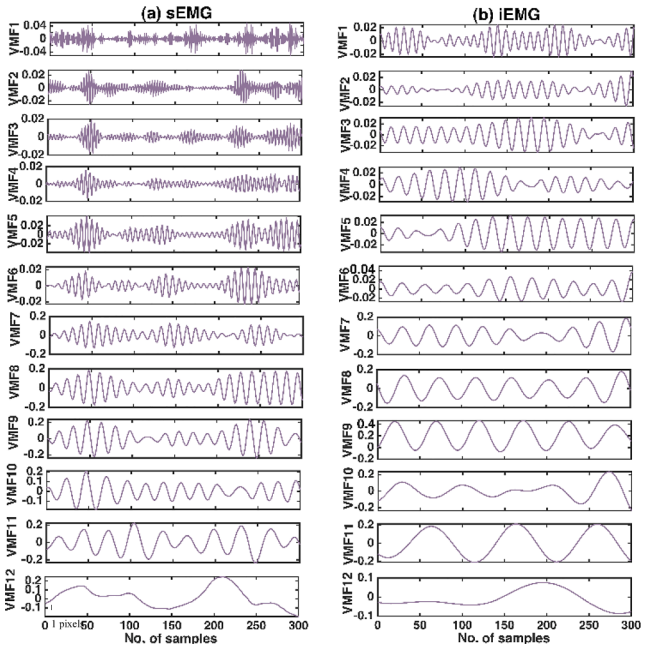

Fig. 7. (a) sEMG signal with respective VMD model functions with added noise of 5db (b) iEMG signal with respective model functions of VMD with added noise of 5db.

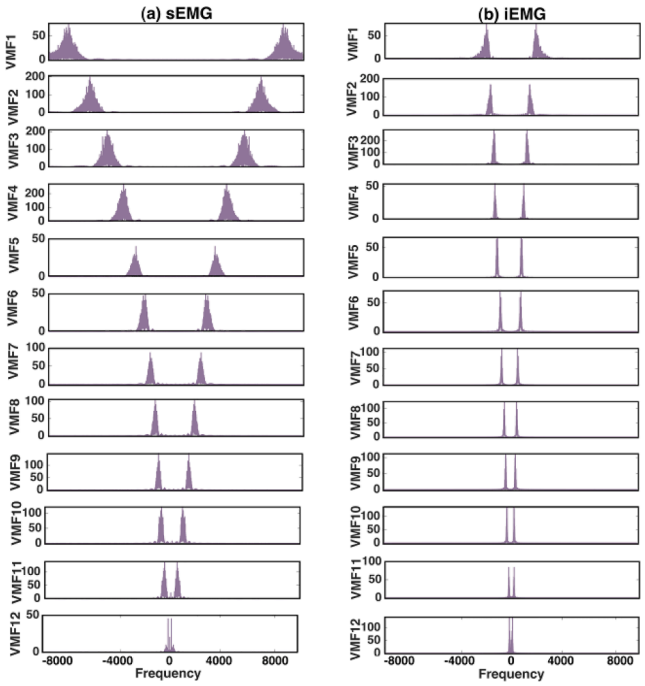

Fig. 8. Frequency spectra of respective modal functions of VMD with added 5db noise for a) sEMG and b) iEMG.

signals [32]. However, it was shown by Xiao et al. (2019) that VMD with IT and SOFT thresholding operator yields the best performance in eliminating noise from sEMG signals [23]. Tables 1 and 2 show the denoising performance of wavelet based denoising, non-local means filter, wiener filter, EMD using IT and SOFT thresholding operator along with VMD using IT (VMD-IT) and IIT (VMD-IIT) with the thresholding operators SOFT (SIIT-VMD), HARD (HIIT-VMD), and SCAD for sEMG and iEMG, respectively.

It is evident that SNR and RMSE values of wavelet based denoising, non-local means filter and wiener filter are poor as compared to other methods. It can be observed from Table 1 that SNR values of denoised sEMG signals with IIT and SOFT thresholding operators are higher than the SNR value corresponding to IT for all the added noise levels. Whereas for iEMG, in the case of noise levels of 10db and 15db SNR values of IT with SOFT thresholding operator are 12.6 and 15.6 which are higher than respective SNR values corresponding to IIT when used with the SOFT thresholding operator. It can also be seen that RMSE values are the lowest corresponding to denoising with IIT and SOFT thresholding operator at all noise levels. Table 3 shows that all of these results are significant.

From Table 2, it is evident for a noise level of 10db, the performance of VMD-IT with an SNR value of 12.7 is better than that of VMD-IIT with an SNR value of 12.6. The same trend can be observed for the noise level of 15db corresponding to both SNR and RMSE. Although the noise levels of VMD-IT of 10db and 15db performed better than VMD-IIT, the SNR and RMSE of both methods are comparable. Table 3 demonstrates the significance of these results.

Figs. 9 and 10 show the comparison of denoised sEMG and iEMG signals, respectively, resulting from IT and IIT. Fig. 9 shows the original sEMG signal, the noisy sEMG signal, and the filtered signals using VMD-IT and VMD-IIT, respectively. Fig. 10 shows the original sEMG signal, the noisy sEMG signal, and the filtered signals using VMD-IT and VMD-IIT respectively. It can be concluded from Figs. 9 and 10 that IIT provides a smoother and closer approximation of the original signal after denoising as it preserves its original characteristics.

From Table 1, it can be observed that the SOFT operator yields the highest output SNR and lowest RMSE at all noise levels for sEMG signals. In the case of iEMG it can be seen from Table 2 that the SOFT operator yields the highest output SNR and lowest RMSE at 0db, 5db, and 10db levels but at a noise level of 15db HARD operator has the highest output SNR and lowest RMSE. Table 4 shows the significance of these obtained values.

Figs. 11, and 12 show the comparison of denoised signals using SOFT, HARD, and SCAD as thresholding operators for sEMG and iEMG respectively. It can be seen that the signal reconstructed using SIIT-VMD is the smoothest approximation of the original signal. As it is evident from Figs. 11 and 12 that the reconstructed signal as a result of HIIT-VMD, contains abrupt changes.

A comparison of the original sEMG and iEMG signal with the denoised EMG signals after adding 5db noise using the proposed method has been shown in Fig. 13 and Fig. 14 respectively. It can be seen that the reconstructed signal preserves the original characteristics of the original signal.

4. Discussion

The paper proposes an SIIT-VMD technique for both sEMG and iEMG referred to as the proposed method. Before this study, no literature has been found that applied VMD-based denoising methods to iEMG. The proposed method provides better results than previously proposed denoising methods based on EMD and VMD [23,32]. Data were collected from 5 healthy subjects simultaneously for sEMG and iEMG. The input signals were decomposed using VMD and introduced with noise at different levels. These noise-contaminated signals were then subjected to denoising using various denoising techniques and operators. VMD was applied in combination with two kinds of thresholding techniques i. e. IT and IIT along with three different thresholding operators (SOFT, HARD, and SCAD).

It can be seen from Fig. 8 that each VMF has a center frequency and narrow bandwidth that becomes narrower in higher-order VMFs. The use of a quadratic penalty in (6) favors denoising and encourages the fidelity of the reconstruction [14], thus providing a higher SNR and a lower RMSE of the reconstructed signal. The obtained modes are searched for center frequencies that can reconstruct the input signal [14,34]. Due to the narrow frequency band and concentrated frequency,

Table 1
Mean signal-to-noise ratio corresponding to surface emg.

	0db	0db	5db	5db	10db	10db	15db	15db
	SNR	**RMSE**	**SNR**	**RMSE**	**SNR**	**RMSE**	**SNR**	**RMSE**
Wavelet Denoising	0.6	1.2	1.3	0.9	1.7	0.8	2.0	0.8
Non-Local Means	1.3	1.0	2.0	0.7	2.2	0.6	2.2	0.6
Weiner Filter	−1.3	1.5	1.4	0.9	2.4	0.6	4.1	0.5
EMD IT SOFT	3.2	0.6	5.9	0.5	8.9	0.3	11.0	0.3
VMD IT SOFT	3.2	0.6	8.5	0.3	14.0	0.2	19.4	0.1
EMD IIT SOFT	3.4	0.6	6.2	0.4	9.2	0.3	11.3	0.3
VMD IIT SOFT	**3.9**	**0.6**	**9.2**	**0.3**	**14.6**	**0.2**	**19.8**	**0.1**
VMD IIT HARD	1.7	0.7	6.9	0.41	12.2	0.2	17.4	0.1
VMD IIT SCAD	2.8	0.7	8.1	0.36	13.6	0.2	19.0	0.1

Table 2
Mean signal-to-noise ratio corresponding to intramuscular emg.

	0db	0db	5db	5db	10db	10db	15db	15db
	SNR	**RMSE**	**SNR**	**RMSE**	**SNR**	**RMSE**	**SNR**	**RMSE**
Wavelet Denoising	0.5	0.7	1.4	0.5	2.1	0.5	2.4	0.4
Non-Local Means	−0.3	0.9	−1.1	0.7	−1.8	0.7	−2.1	0.7
Weiner Filter	−0.01	1.0	1.1	0.8	1.4	0.6	1.5	0.5
EMD IT SOFT	1.4	0.5	2.2	0.4	2.6	0.4	2.6	0.4
VMD IT SOFT	3.1	0.4	8.3	0.2	12.7	0.1	15.7	0.1
EMD IIT SOFT	1.5	0.5	2.2	0.4	2.7	0.4	2.9	0.4
VMD IIT SOFT	**3.7**	**0.4**	**8.7**	**0.2**	**12.7**	**0.1**	15.1	0.1
VMD IIT HARD	1.7	0.5	6.9	0.2	11.6	0.1	**15.3**	**0.1**
VMD IIT SCAD	2.7	0.4	8.0	0.2	12.3	0.1	15.2	0.1

Both tables contain mean SNR values calculated from 5 subjects. The bold cells have the highest SNR values.

Table 3
statistical results of the denoising performance for vmd-it and vmd-iit.

Noise Level	sEMG	iEMG
0 dB	≤0.05	≤0.05
5 dB	≤0.05	≤0.05
10 dB	≤0.05	≥0.05
15 dB	≤0.05	≤0.05

the elimination of noise becomes easier [14,35] making VMD better than EMD and wavelet decomposition for denoising. Furthermore, it was concluded by [36] that EMD is sensitive to noise, qualifying VMD for better denoising performance. The results in Tables 1 and 2 show that

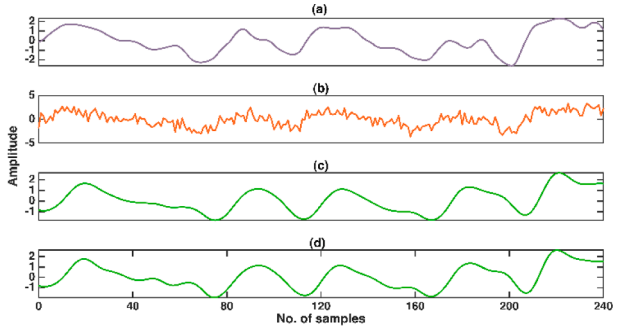

Fig. 9. Comparison between original sEMG, noisy sEMG, and denoised signals using VMD-IT and VMD-IIT. (a) Original signal; (b) Signal with noise, (c) Denoised signal using VMD-IT (d) Denoised signal using VMD-IIT.

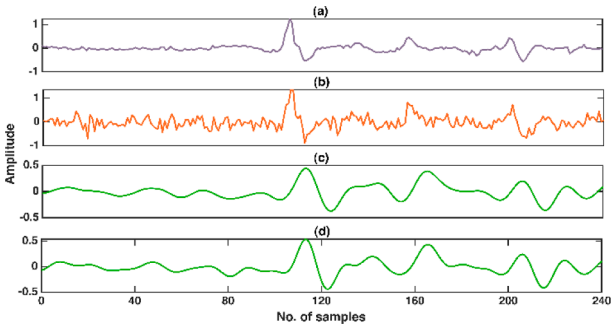

Fig. 10. Comparison between original iEMG, noisy iEMG, and denoised signals using VMD-IT and VMD-IIT. (a) The original signal, (b)Signal with noise, (c) Denoised signal using VMD-IT, (d) Denoised signal using VMD-IIT.

Table 4
Statistical results of the denoising performance for soft, hard, and scad.

Noise Level	sEMG			iEMG		
	SOFT & HARD	SOFT & SCAD	HARD & SCAD	SOFT & HARD	SOFT & SCAD	HARD & SCAD
0 dB	≤0.05	≤0.05	≤0.05	≤0.05	≤0.05	≤0.05
5 dB	≤0.05	≤0.05	≤0.05	≤0.05	≤0.05	≤0.05
10 dB	≤0.05	≤0.05	≤0.05	≤0.05	≤0.05	≤0.05
15 dB	≤0.05	≤0.05	≤0.05	≤0.05	≤0.05	≥0.05

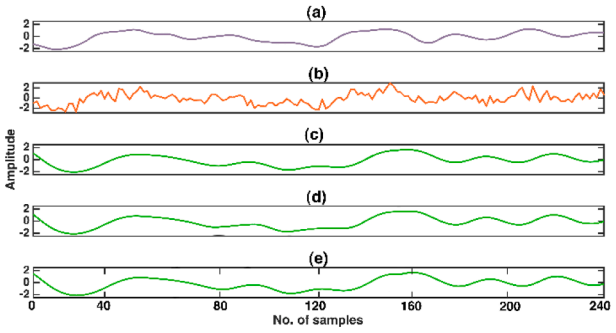

Fig. 11. Comparison between SOFT, HARD, and SCAD operators for sEMG. (a) The original signal, (b) Noisy signal, (c) Denoised signal using SOFT operator, (d) Denoised signal using HARD operator, (e) Denoised signal using SCAD operator.

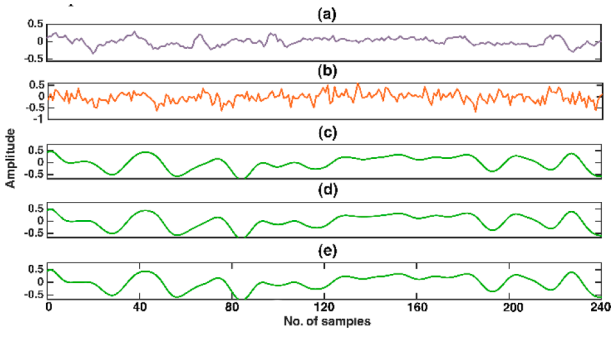

Fig. 12. Comparison between SOFT, HARD, and SCAD operators for iEMG. (a) The original signal, (b) Noisy signal, (c) Denoised signal using SOFT operator, (d) Denoised signal using HARD operator, (e) Denoised signal using SCAD operator.

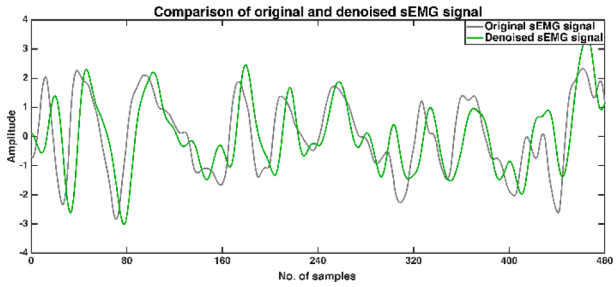

Fig. 13. Comparison between the original and denoised signal for sEMG.

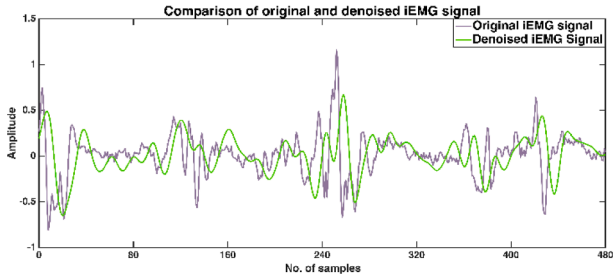

Fig. 14. Comparison between the original and denoised signal for iEMG.

VMD outperforms EMD for both thresholding techniques.

Invasive recording of the iEMG signal results in the recording of other spontaneous activities that occur around the muscles such as fibrillation occurring due to denervation. The recording of such activities affects the iEMG signal causing rapid fluctuations in the signal. EMD is an empirical method lacking any mathematical basis and has the disadvantage of mode mixing due to intermittency signals and noise [36]. Due to the highly non-stationary iEMG signal, mode mixing becomes more dominant and EMD fails to preserve the original characteristics of the signal. As VMD has a mathematical basis and is not entirely dependent on the data, the issue of mode mixing is resolved [13]. Thus, the proposed method is prevalent and has the flexibility to be used for both sEMG and iEMG.

The thresholding techniques IT and IIT, used in this study, are inspired and developed from translation-invariant wavelet thresholding. Both IT and IIT were used after decomposing the input signal using VMD into its respective VMFs. The IIT thresholding technique averages the different versions of the denoised signal produced iteratively thus providing better tolerance against noise [34]. The values obtained corresponding to VMD-IIT for SNR are higher and for RMSE are lower in the case of all added noise levels for sEMG as shown in Table 1. Statistical analysis also shows that the two techniques exhibit a significant difference (P-value < 0.05). Although VMD-IIT proved to provide better results for sEMG at noise levels 0db, 5db, 10db, and 15db, SNR and RMSE obtained at different noise levels showed a varied trend for iEMG. The results obtained at 0db and 5db show the same trend as sEMG, but at 10db and 15db, the SNR value for VMD-IT was higher than VMD-IIT as depicted in Table 2. The statistical analysis does not show any significant difference between the two techniques for iEMG at 10db, as shown in Table 3.

Out of the three thresholding operators used, SIIT-VMD provided the best SNR and RMSE of the reconstructed signal. SIIT-VMD overcomes the issue of signal discontinuity that occurs in the case of HIIT-VMD due to the use of a HARD thresholding operator [35]. As evident from Table 2, a SOFT operator at all noise levels for both iEMG and sEMG provides the best SNR and RMSE values. Statistical analysis shows a significant difference between the three operators for sEMG. For iEMG, statistical analysis shows that there is a significant difference between the three operators but at a noise level of 15db, a significant difference is

Table 5
Comparison of the percentage increase in the snr values of the proposed method with previously proposed methods.

SNR	Proposed Method	Ashraf et al. [32]	Xiao et al. [23]
5 dB	83.7 %	110.3 %	115.3 %
10 dB	46.3 %	35.2 %	44.0 %
15 dB	32.3 %	2.8 %	0.3 %

not present between SCAD and HARD operator. However, the results show a significant difference between SOFT and the remaining two operators at all noise levels, as demonstrated in Table 4. Therefore, the SIIT-VMD method has the best denoising performance for sEMG and iEMG.

Table 5 shows the comparison of the proposed denoising method with previously proposed methods [23,32]. The table shows the percentage increase in the SNR value of denoised signals compared to the noisy signal at three different noise levels. It is evident from Table 5 that the percentage increase by the proposed denoising method is highest for 10db and 15db while providing a lower increment in the SNR value at a noise level of 5db. The noise introduced at the 5db level introduces more noise components as compared to 10db and 15db thus providing a lower increment of SNR. This occurs due to higher non-stationarity thus resulting in lower SNR as compared to EMD-IT and SIT proposed by Ashraf et al. (2021) [32] and Xiao et al. (2019) [23], respectively. The method is general and flexible enough to be applied to both sEMG and iEMG but the previously proposed methods based on EMD and VMD [23,32] were not applied to iEMG.

The proposed method can be used for the extraction of time–frequency domain features in the future that will provide more useful information about electromyography data. These findings can be implemented in the initial stages of development of practical applications such as disease diagnosis [37], multiday evaluation of iEMG [38], limb movement classification [39], motion intention identification [40], human–machine interaction [41] and motion detection. This SIIT-VMD denoising method can also be applied for applications such as the assessment of spasticity, checking the continuity of the signal, and gesture recognition.

The disadvantages of VMD include the requirement of a predefined number of modes for decomposition [14]. Moreover, VMD is unable to separate the DC component in a signal and does not handle high levels of non-stationarity such as sudden signal onset [14]. The SOFT operator results in the shift of the signal by an amount of a predefined threshold value. Therefore, SIIT-VMD can cause an unnecessary bias in the resulting signal and can be more computationally complex as it is an iterative method [32]. In the future, a study should be carried out to compare the denoising performance of the proposed method for concentric and eccentric isotonic motions.

5. Conclusion

The study aimed to assess the performance of VMD for denoising of sEMG and iEMG. The study proposes a denoising technique with the best performance after decomposing the signals obtained from 5 healthy subjects, into respective VMFs using VMD. Two thresholding techniques, IT and IIT, were utilized in combination with three thresholding operators (SOFT, HARD, and SCAD) to denoise the decomposed signal. The results proved that the SOFT thresholding operator with the IIT thresholding technique provides the best approximation of the original signal without altering the original characteristics of the signal. SIIT-VMD can be used for denoising sEMG as well as for iEMG preserving the original characteristics of the signals.

This work was supported by Higher Education Commission (HEC) of Pakistan for funding this project under grant# 10238/Federal/NPRU/RD/HEC/2017.

CRediT authorship contribution statement

H. Ashraf: Conceptualization, Data curation, Formal analysis, Software, Writing – review & editing. **U. Shafiq:** Formal Analysis, Software, Methodology, Writing - original draft, Writing - review & editing Validation, Visualization. **Q. Sajjad:** Writing - review & editing, Investigation. **A. Waris:** Funding acquisition, Supervision, Project administration. **O. Gilani:** Resources, Validation, Supervision. **M. Boutaayamou:** Writing - review & editing, Supervision **O. Brüls:** Writing - review & editing, Supervision.

Declaration of Competing Interest

The authors declare that this work was supported by Higher Education Commission (HEC) of Pakistan for funding this project under grant# 10238/Federal/NPRU/RD/HEC/2017.

Data availability

Data will be made available on request.

References

[1] J. Chen, X. Zhang, Y. Cheng and N. Xi, “Surface EMG based continuous estimation of human lower limb joint angles by using deep belief networks”, Biomedical Signal Processing and Control, vol. 40, pp. 335-342, 2018. Available: 10.1016/j.bspc.2017.10.002 [Accessed 23 February 2022].
[2] J. Fagundes, D. Cantergi, F. Milman, M. La and C. Tarrago, “Evaluating the Electromyographical Signal During Symmetrical Load Lifting”, Applications of EMG in Clinical and Sports Medicine, 2012. Available: 10.5772/25732 [Accessed 23 February 2022].
[3] D. Farina, D. Stegeman, R. Merletti, Biophysics of the Generation of EMG Signals, Surface Electromyography: Physiology, Engineering, and Applications, pp. 1-24, 2016. Available: 10.1002/9781119082934.ch02 [Accessed 23 February 2022].
[4] I. Campanini, C. Disselhorst-Klug, W. Rymer and R. Merletti, Surface EMG in Clinical Assessment and Neurorehabilitation: Barriers Limiting Its Use, Front. Neurol. 11 (2020). Available: 10.3389/fneur.2020.00934 [Accessed 23 February 2022].
[5] A. Asif, A. Waris, S. Gilani, M. Jamil, H. Ashraf, M. Shafique, I. Niazi, Performance evaluation of convolutional neural network for hand gesture recognition using EMG, Sensors 20 (6) (2020) 1642.
[6] R. Merletti, D. Farina, Analysis of intramuscular electromyogram signals, Philos. Trans. Royal Soc. A: Math. Phys. Eng. Sci.367(1887) (2008) 357–368, 2008. Available: 10.1098/rsta.2008.0235 [Accessed 23 February 2022].
[7] J. Wang, L. Tang, J.E Bronlund, Surface EMG Signal Amplification and Filtering, International Journal of Computer Applications 82(1) (2013) 15-22, 2013. Available: 10.5120/14079-2073 [Accessed 23 February 2022].
[8] A. Andrade, S. Nasuto, P. Kyberd, C. Sweeney-Reed, F. Van Kanijn, EMG signal filtering based on Empirical Mode Decomposition, Biomed. Signal Process. Control 1(1) (2006) 44-55. Available: 10.1016/j.bspc.2006.03.003 [Accessed 23 February 2022].
[9] J. Maier, A. Naber, M. Ortiz-Catalan, Improved prosthetic control based on myoelectric pattern recognition via wavelet-based de-noising, in: IEEE Transactions on Neural Systems and Rehabilitation Engineering 26(2) (2018) 506-514. Available: 10.1109/tnsre.2017.2771273 [Accessed 23 February 2022].
[10] X. Ren, Z. Yan, Z. Wang, X. Hu, Noise reduction based on ICA decomposition and wavelet transform for the extraction of Motor Unit Action Potentials, J. Neurosci. Methods 158 (2) (2006) 313–322.
[11] C. Zhang, T. Sun, Discussion of the influence of multiscale PCA denoising methods with three different features, Sensors 22 (4) (2022) 1604.
[12] N. Huang et al., The empirical mode decomposition and the Hilbert spectrum for nonlinear and non-stationary time series analysis, Proc. Roy. Soc. Lond. Series A: Math. Phys. Eng. Sci. 454 (1998) 1971: 903-995, 1998. Available: 10.1098/rspa.1998.0193 [Accessed 23 February 2022].
[13] H. Ge, G. Chen, H. Yu, H. Chen, F. An, Theoretical analysis of empirical mode decomposition, Symmetry 10(11) (2018) 623. Available: 10.3390/sym10110623 [Accessed 23 February 2022].
[14] K. Dragomiretskiy, D. Zosso, Variational mode decomposition, in: IEEE Transactions on Signal Processing, vol. 62, no. 3, pp. 531-544, 2014. Available: 10.1109/tsp.2013.2288675 [Accessed 23 February 2022].
[15] Z. Wu, N. Huang, Ensemble Empirical Mode Decomposition: A Noise-Assisted Data Analysis Method, Advances in Adaptive Data Analysis, vol. 01, no. 01, pp. 1-41, 2009. Available: 10.1142/s1793536909000047 [Accessed 23 February 2022].
[16] M.E. Torres, M.A. Colominas, G. Schlotthauer, P. Flandrin, A complete ensemble empirical mode decomposition with adaptive noise, 2011 IEEE International Conference on Acoustics, Speech and Signal Processing (ICASSP), 2011, pp. 4144-4147, doi: https://doi.org/10.1109/ICASSP.2011.5947265.

[17] Variational mode decomposition, Variational Mode Decomposition - an overview | ScienceDirect Topics. [Online].Available:www.sciencedirect.com/topics/engineering/variational-mode-decomposition [Accessed: 23-Feb-2022].
[18] G. Li, G. Tang, G. Luo, H. Wang, Underdetermined blind separation of bearing faults in hyperplane space with variational mode decomposition, Mechanical Systems and Signal Processing, vol. 120, pp. 83-97, 2019. Available: 10.1016/j.ymssp.2018.10.016 [Accessed 23 February 2022].
[19] K. Hong, L. Wang, S. Xu, A variational mode decomposition approach for degradation assessment of power transformer windings, IEEE Trans. Instrum. Meas. 68 (4) (2019) 1221–1229, https://doi.org/10.1109/TIM.2018.2865048.
[20] Q. Wang, C. Yang, H. Wan, D. Deng, A. Nandi, Bearing fault diagnosis based on optimized variational mode decomposition and 1D convolutional neural networks, Meas. Sci. Technol. 32 (10) (2021), 104007.
[21] S. Lahmiri, M. Boukadoum, Biomedical image denoising using variational mode decomposition. 2014 IEEE Biomedical Circuits and Systems Conference (BioCAS) Proceedings, 2014.
[22] P. Singh, G. Pradhan, Variational mode decomposition based ECG denoising using non-local means and wavelet domain filtering, Australas. Phys. Eng. Sci. Med. 41 (4) (2018) 891–904.
[23] F. Xiao, D. Yang, X. Guo, Y. Wang, VMD-based denoising methods for surface electromyography signals, J. Neural Eng. 16 (5) (2019), 056017.
[24] S. Ma, B. Lv, C. Lin, X. Sheng and X. Zhu, "EMG Signal Filtering Based on Variational Mode Decomposition and Sub-Band Thresholding", IEEE Journal of Biomedical and Health Informatics, vol. 25, no. 1, pp. 47-58, 2021. Available: https://doi.org/10.1109/jbhi.2020.2987528 [Accessed 23 February 2022].
[25] G. Lu, J.-S. Brittain, P. Holland, J. Yianni, A.L. Green, J.F. Stein, T.Z. Aziz, S. Wang, Removing ECG noise from surface EMG signals using adaptive filtering, Neurosci. Lett. 462 (1) (2009) 14–19.
[26] Z. Sun, X. Xi, C. Yuan, Y. Yang, X. Hua, Surface electromyography signal Denoising via EEMD and improved wavelet thresholds, Math. Biosci. Eng. 17 (6) (2020) 6945–6962.
[27] X. Xi, Y. Zhang, Y. Zhao, Q. She, Z. Luo, Denoising of surface electromyogram based on complementary ensemble empirical mode decomposition and improved interval thresholding", Review of Scientific Instruments, vol. 90, no. 3, p. 035003, 2019. Available: https://doi.org/10.1063/1.5057725 [Accessed 21 March 2022].
[28] E.N. Kamavuako, et al., On the usability of intramuscular EMG for prosthetic control: A Fitts' law approach, J. Electromyography Kinesiol. 24 (Oct. 2014) 770–777.
[29] R. Rockafellar, A dual approach to solving nonlinear programming problems by unconstrained optimization, Mathematical Programming, vol. 5, no. 1, pp. 354-373, 1973. Available: https://doi.org/10.1007/bf01580138 [Accessed 21 March 2022].
[30] M. Hestenes, Multiplier and gradient methods, J. Optimization Theory Appl., vol. 4, no. 5, pp. 303-320, 1969. Available: 10.1007/bf00927673 [Accessed 21 March 2022].
[31] Y. Kopsini,s S. McLaughlin, Empirical mode decomposition based denoising techniques, 1st international work-shop on cognitive information processing (CIP), Jun. 2008.
[32] H. Ashraf, A. Waris, S.O. Gilani, M.U. Tariq, H. Alquhayz, Threshold Parameters Selection for Empirical Mode Decomposition-Based EMG Signal Denoising, Intelligent Automation Soft Computing 27 (3) (2021) 799–815.
[33] A. Waris, I.K. Niazi, M. Jamil, K. Englehart, W. Jensen, et al., Multiday evaluation of techniques for EMG based classification of hand motions, IEEE J. Biomed. Health Inform. 23 (4) (2018) 1526–1534.
[34] S. Lahmiri, A. Shmuel, Variational mode decomposition based approach for accurate classification of color fundus images with hemorrhages, Opt. Laser Technol. 96 (2017) 243–248.
[35] U. Raghavendra et al., "Automated screening of congestive heart failure using variational mode decomposition and texture features extracted from ultrasound images", Neural Computing and Applications, vol. 28, no. 10, pp. 2869-2878, 2017. Available: https://doi.org/10.1007/s00521-017-2839-5 [Accessed 21 March 2022].
[36] M. Zhou et al., De-noising of photoacoustic sensing and imaging based on combined empirical mode decomposition and independent component analysis", Journal of Biophotonics, vol. 12, no. 8, 2019. Available: https://doi.org/10.1002/jbio.201900042 [Accessed 1 February 2022].
[37] S. Becker, S. von Werder, A. Lassek and C. Disselhorst-Klug, "Time-frequency coherence of categorized sEMG data during dynamic contractions of biceps, triceps, and brachioradialis as an approach for spasticity detection", Medical & Biological Engineering & Computing, vol. 57, no. 3, pp. 703-713, 2018. Available: https://doi.org/10.1007/s11517-018-1911-3 [Accessed 31 January 2022].
[38] A. Waris, M. Zia ur Rehman, I. Niazi, M. Jochumsen, K. Englehart, W. Jensen, H. Haavik and E. Kamavuako, 2020. A Multiday Evaluation of Real-Time Intramuscular EMG Usability with ANN. Sensors, 20(12), p.3385.
[39] P. Shull, S. Jiang, Y. Zhu and X. Zhu, "Hand Gesture Recognition and Finger Angle Estimation via Wrist-Worn Modified Barometric Pressure Sensing", IEEE Transactions on Neural Systems and Rehabilitation Engineering, vol. 27, no. 4, pp. 724-732, 2019. Available: https://doi.org/10.1109/tnsre.2019.2905658.
[40] F. Xiao, Y. Wang, Y. Gao, Y. Zhu and J. Zhao, "Continuous estimation of joint angle from electromyography using multiple time-delayed features and random forests", Biomedical Signal Processing and Control, vol. 39, pp. 303-311, 2018. Available: https://doi.org/10.1016/j.bspc.2017.08.015 [Accessed 1 February 2022].
[41] F. Xiao, "Proportional myoelectric and compensating control of a cable-conduit mechanism-driven upper limb exoskeleton", ISA Transactions, vol. 89, pp. 245-255, 2019. Available: https://doi.org/10.1016/j.isatra.2018.12.028 [Accessed 1 February 2022].